RSC Mechanochemistry

ROYAL SOCIETY OF CHEMISTRY

PAPER

View Article Online
View Journal

Cite this: DOI: 10.1039/d5mr00118h

Mechanochemical synthesis of aspirin nanocrystals for pharmaceutical applications

G. D. S. Kanchana Garumanna, [ab] Ranjit Thakuria [cd] and Nadeesh M. Adassooriya *[ab]

Aspirin's oral bioavailability is about 50%, but this can be significantly improved through nanocrystal formulation and polymorphic transformation. However, achieving homogeneous nanocrystals with optimal stability and morphology remains challenging. In this study, pure aspirin was synthesized chemically, and nanocrystals were generated using both neat grinding (NG) and liquid-assisted grinding (LAG). Key parameters such as nature of liquid, liquid-to-solid ratio (η), milling frequency, milling time, and temperature were systematically optimized. Both solution crystallisation and mechanochemical milling successfully produced Form IV, which remains stable for over 60 days under ambient conditions (22–27 °C and 45–75% RH). Using water as the added liquid consistently converts aspirin Form IV to stable Form I under η = 0.07–0.15, 30 Hz and 10–120 minutes of milling. With cyclohexane, Form IV transforms to Form I within 30 minutes at η = 0.1, but reverts to Form IV after 60 minutes, and increasing η maintains it in Form IV for a period of over 60 days. Optimal nanocrystals were obtained by milling at 30 Hz for 30 minutes around 28 °C, with η between 0.1 and 0.2. Water proves to be most effective, as its hydrogen bonding disrupts the aspirin crystal lattice, and high surface tension improves shear stress transfer. This yields nanocrystals of ~150 nm, reduces the melting point by 25.1 °C, and achieves ~90% drug release within 6.5 minutes at pH 1.2, highlighting the potential of aspirin nanocrystals for enhanced bioavailability and therapeutic performance.

Received 16th September 2025
Accepted 14th February 2026

DOI: 10.1039/d5mr00118h

rsc.li/RSCMechanochem

1 Introduction

One of the main limitations in the pharmaceutical use of aspirin, as with many active pharmaceutical ingredients (APIs), is its poor water solubility, which reduces bioavailability (~40–50%) and weakens therapeutic performance.[1,2] This issue affects nearly 70% of new drug candidates, creating major challenges in formulation, efficacy, and safety.[1] Aspirin, or acetylsalicylic acid (ASA), remains one of the most widely used pharmaceuticals. Aspirin, an organic compound first synthesized in 1899, has a medicinal history extending over 3500 years, with its origins traced to the traditional use of willow bark as an analgesic and antipyretic.[3–5]

To address this, various solubilization strategies have been explored, including chemical modification, complexation, and the use of surfactants and co-solvents.[2] Among them, nanocrystal-based drug delivery systems have gained attention for enhancing the solubility and bioavailability of poorly soluble drugs.[6] Made almost entirely of the active drug, or with minimal surfactant, nanocrystals improve dissolution rates and dose uniformity and reduce food-related effects and toxicity.[7,8] These systems are particularly valuable for BCS (Biopharmaceutics Classification System) Class II and IV drugs, improving both pharmacokinetics and pharmacodynamics.[6,7,9,10] Nanocrystals can be administered *via* oral, ophthalmic, dermal, parenteral, and pulmonary routes and have shown better skin permeation and therapeutic effects in dermal applications.[6,9]

Nanocrystals are typically produced using top-down methods like milling or bottom-up approaches such as precipitation.[7] Mechanochemical milling has become a sustainable and scalable technique for pharmaceutical synthesis, requiring little to no solvent.[11,12] It is effective for producing APIs and novel solid forms like polymorphs, cocrystals, and salts,[12,13] offering faster processing, fewer steps, and higher throughput than traditional methods.[11,14] Its ability to generate nanocrystals under ambient conditions and on a kilogram scale makes it ideal for industrial use.[14] Recent advances include *in situ* monitoring and dendrimer-based nanocrystals for improved drug delivery.[15]

Polymorphism, however, significantly influences therapeutic outcomes. Aspirin polymorph II, first structurally characterized in 2005 after being predicted by crystal structure prediction

[a]*Department of Chemical and Process Engineering, Faculty of Engineering, University of Peradeniya, Peradeniya 20400, Sri Lanka. E-mail: nadeeshm@eng.pdn.ac.lk; kanchanagarumanna@gmail.com; kanchanag@eng.pdn.ac.lk*

[b]*Postgraduate Institute of Science, University of Peradeniya, P. O. Box 25, Peradeniya, Sri Lanka*

[c]*Department of Chemistry, Gauhati University, Guwahati 781014 Assam, India. E-mail: ranjit.thakuria@gmail.com; ranjit.thakuria@gauhati.ac.in*

[d]*Faculty of Chemistry, University of Warsaw, 1 Pasteura Street, 02-093 Warsaw, Poland*

(CSP) methods,[16] was isolated in pure form only in 2011.[17] A third form, aspirin III, appears at pressures above 2 GPa, showing distinct Raman spectral changes, though its structure remains unsolved due to instability at room temperature.[18] Form IV, discovered in 2017 *via* powder X-ray diffraction and Raman spectral changes, is metastable and is synthesised *via* melt crystallization and reverts to Form I within minutes at room temperature. Its stability can be extended up to an hour with additives like Canada balsam, polyvinylpyrrolidone, or mannitol, and up to 24 hours at 4 °C.[19] Hence, aspirin exhibits four known polymorphic forms (Forms I, II, III,[18] and IV[19]), each characterized by distinct Raman spectral features. Among them, Form III displays the most pronounced spectral variations, while Forms I, II and IV show relatively similar Raman spectra. Nevertheless, significant differences in their spectral profiles confirm the presence of four distinct polymorphs. Furthermore, Forms I, II, and IV exhibit well-defined XRD patterns, enabling clear differentiation based on crystallographic data.

This study explores the mechanochemical synthesis and detailed characterization of aspirin nanocrystals. Key process parameters such as nature of liquid additives, liquid-to-solid ratio (η), milling time, frequency, and temperature were optimized under NG and LAG conditions. Special focus was placed on polymorphic transitions during milling and on drug release in simulated gastrointestinal environments. The goal is to highlight the potential of aspirin nanocrystals to improve oral bioavailability and therapeutic performance.

2 Experimental section

2.1 Materials

Ethanol (99.96%, VWR International, France), salicylic acid (≥99%, Research Lab Fine Chem Industries), acetic anhydride (>96%, DAEJUNG, CAS No: 108-24-7), and deionized water were used without further purification. Tetrahydrofuran, cyclohexane, acetonitrile and dichloroethane (99.5%, Central Drug House), acetone, toluene and hexane (≥99%, Sigma-Aldrich), HCl and H_2SO_4 (≥98%, Sigma-Aldrich), and NaCl, KH_2PO_4 and Na_2HPO_4 (≥99%, Sigma-Aldrich) were used.

2.2 Experimental design

2.2.1 Chemical synthesis of aspirin. Aspirin was synthesized by reacting 5 g of salicylic acid with 4.5 mL of acetic anhydride, followed by stirring at 500 rpm for 5 minutes at 27 °C. Five drops of concentrated H_2SO_4 were added, and the mixture was heated at 70–75 °C for 18 minutes under continuous stirring. The reaction was quenched with 60 mL of ice-cold distilled water and further cooled in an ice bath for 10 minutes. The precipitate was collected *via* vacuum filtration and recrystallized using absolute ethanol and cold water. Purified crystals were dried in a desiccator and characterized by a ferric chloride test, thermogravimetric analysis (TGA), Fourier transform infrared (FTIR), and powder X-ray diffraction (PXRD).

2.2.2 Aspirin nanocrystal synthesis. Nanocrystals of aspirin were synthesized using NG and LAG. The grinding process was carried out using a vibratory mill (Retsch MM 400) equipped with two 25 mL jars and two stainless steel balls of 10 mm diameter for each.

2.2.3 Optimisation of nanocrystal synthesis. Processing parameters were systematically optimized by evaluating various liquids: tetrahydrofuran, hexane, cyclohexane, toluene, acetonitrile, ethanol, distilled water, dichloromethane, and acetone, using 500 mg of aspirin with η values ranging from 0.1 to 0.4. Each mixture was milled at 30 Hz for 60 minutes at 26–28 °C under ambient air. Further optimization included varying milling time (10–120 minutes), adjusting frequency (20, 25, and 30 Hz), and monitoring jar air temperature and relative humidity before and after milling using a Hygro-Thermometer (Gondo, HT-390 EZODO).

2.2.4 Ferric chloride colorimetric analysis of aspirin. A 1.0% w/v ferric chloride solution was prepared by dissolving 100.0 mg of $FeCl_3 \cdot 6H_2O$ in 10 mL of distilled water. The test solution was prepared by dispersing 10 mg of the synthesized aspirin in 1 mL of ethanol, followed by the addition of 4 mL of distilled water and gentle mixing to obtain a uniform solution. For the colorimetric analysis, 3–5 mL of the $FeCl_3$ solution was added directly to the prepared test solution and mixed thoroughly at room temperature. The resulting mixture was observed visually for any colour change within 1–10 min.

2.2.5 Aspirin solubility test. Solubility studies of aspirin were carried out using a known mass of the sample. The solid was dispersed in a selected solvent and stirred magnetically in a closed vessel at approximately 27 °C for 3 h, while maintaining a small excess of undissolved material to ensure saturation. The suspension was then allowed to stand for 24 h to reach equilibrium and to confirm the saturation point. After 24 h, the presence of residual solid indicated saturated conditions. The undissolved fraction was separated by filtration using filter paper and air-dried in a bell jar. The mass of the remaining solid was measured, and the total solubility of aspirin was calculated from the difference between the initial mass and the recovered residual mass.

2.2.6 Drug release study of the synthesized aspirin nanocrystals. Drug release studies of aspirin nanocrystals and bulk aspirin were performed in pH 1.2 (simulated gastric fluid) and pH 6.8 (simulated intestinal fluid) buffer solutions, using 200 mL per vessel. The pH 1.2 buffer was prepared using HCl, distilled water, and 2.0 g of NaCl, while the pH 6.8 buffer was formulated with KH_2PO_4, Na_2HPO_4, and distilled water, and dissolution was carried out at 37 ± 0.5 °C with stirring at 100 rpm. A 50 mg dose was introduced under sink conditions, and samples were collected over 3 hours at set intervals. Aliquots (5 mL) were withdrawn, filtered (0.45 μm), and replaced to maintain volume. Drug concentrations were measured *via* UV-Vis spectrophotometry at 275 nm, using pre-established calibration curves (0.5 mg mL^{-1} for pH 1.2; 8.94 mg mL^{-1} for pH 6.8).

2.3 Characterization

PXRD patterns of all synthesized samples were recorded using a Bruker D8 Advanced Eco Powder X-ray diffractometer with Cu Kα radiation ($\lambda = 0.154$ nm) over a 2θ range of 2–80°, with a step

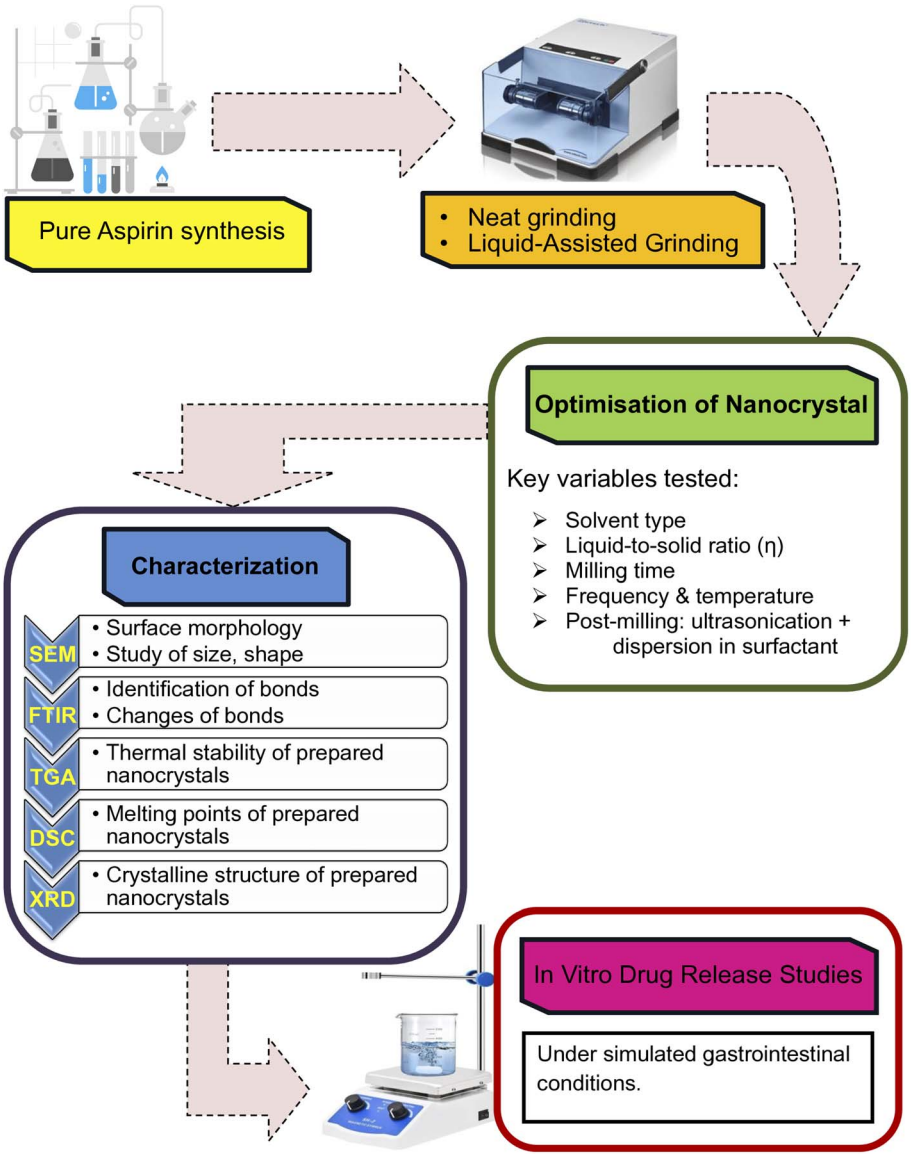

Fig. 1 Schematic representation of the experimental methodology used in this study, including material preparation, milling process, characterization techniques, and release studies.

size of 0.02° and a step time of 0.5 s. The particle size and morphology of the synthesized samples were examined using a Zeiss EVO LS15 scanning electron microscope (SEM). Ground samples were mounted on adhesive carbon tape attached to SEM stubs and coated with a thin layer of gold prior to imaging. The chemical bonding nature of the synthesized samples was analysed using a PerkinElmer Spectrum Two Version 10.6.2 Fourier Transform Infrared (FTIR) spectrometer in the range of 400–4000 cm^{-1}. Thermal behaviour was studied *via* thermogravimetric analysis (TGA) using a PerkinElmer TGA 4000. Samples (10–15 mg) were heated from 40 to 800 °C at a rate of 10 °C min^{-1} under a nitrogen flow (100 cm^3 min^{-1}). Differential Scanning Calorimetry (DSC) analysis was conducted using a TA-SDT 650 (Discovery Series) calorimeter. Measurements were performed from 27.294 to 250.0 °C at a heating rate of 5 °C min^{-1} using a 90 µl alumina pan. The calorimeter was calibrated prior to use to ensure temperature accuracy within ±0.2 °C. Temperature and relative humidity were measured using a Hygro-Thermometer (Gondo, HT-390 EZODO). Absorbance was determined using a HACH (DR 6000) UV-Visible spectrophotometer. Colorimetric analysis using ferric chloride was performed to assess the presence of residual salicylic acid in the synthesized aspirin (see SI, Fig. S6) (Fig. 1).

3 Results and discussion

3.1 Laboratory synthesis of aspirin

The pure aspirin crystals (5–20 µm) exhibit rod- and spike-like morphologies (Fig. 2b). Their successful formation was confirmed by PXRD (Fig. 2a), FTIR, TGA analyses, and colorimetric analysis (see SI, Fig. S2, S3 and S6). Based on a combination of data from the Cambridge Structural Database (CSD)

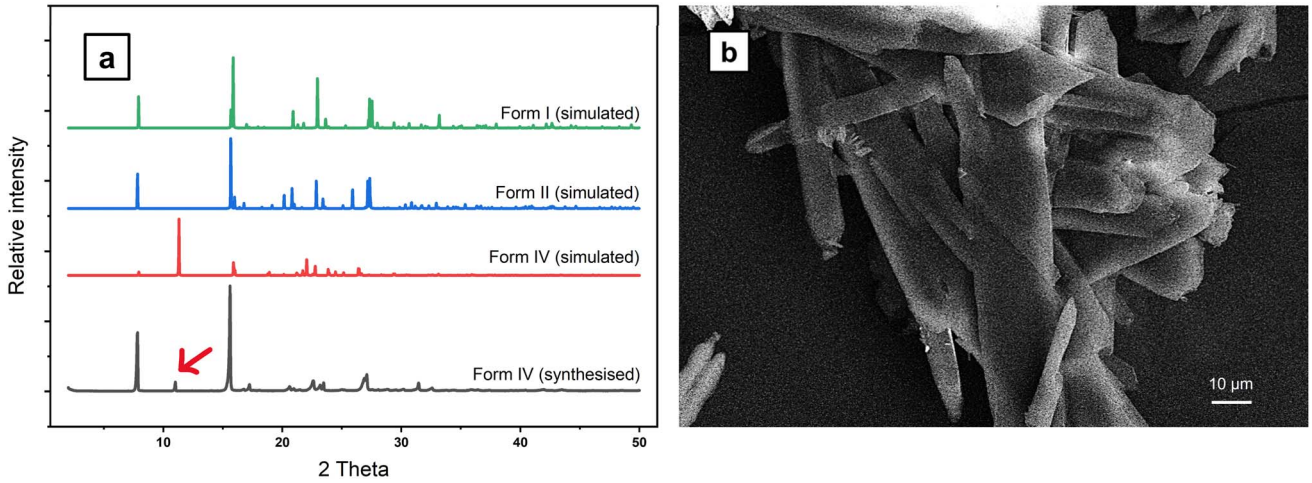

Fig. 2 (a) X-ray powder diffraction patterns of forms I and II (simulated from CSD_CIF_ACSALA02), IV (simulated from CCDC 1541529), and chemically synthesised IV and (b) SEM images of pure aspirin crystals (synthesised).

and Shtukenberg *et al.* (2017),[19] we identified the synthesized form of aspirin as Form IV. The presence of a significant fraction of aspirin Form IV can be confirmed based on a comparison of the simulated and synthesized PXRD patterns. In both cases, a distinct diffraction peak is observed at around $2\theta \approx 11°$, corresponding to the (220) crystallographic plane, which is a characteristic feature of Form IV and is notably absent in Forms I and II. This reflection therefore serves as a reliable diagnostic peak for identifying Form IV within the sample. Quantitative phase analysis was further attempted using Rietveld refinement; however, a reliable distinction between Forms I and IV could not be achieved. This limitation arises from the high structural similarity between these two polymorphs, which leads to extensive overlap and matching of their diffraction peaks. In addition, slight peak shifts are observed in some of the experimental patterns, which may be attributed to lattice strain, crystallite size effects, or minor instrumental and sample preparation variations.

3.2 Liquid-assisted grinding (LAG) experiment

3.2.1 Selection of liquid additives. The liquid additives tested included tetrahydrofuran, hexane, cyclohexane, toluene, acetonitrile, ethanol, water, dichloromethane, and acetone. Among the nine liquids tested, hexane (relative polarity 0.009), cyclohexane (0.006), and water (1.000)[20] were most effective, producing particles of ~200 nm (hexane and cyclohexane) and ~150 nm (water). Water, being highly polar, forms strong hydrogen bonds and transfers shear energy efficiently, aiding controlled fragmentation and preventing agglomeration despite aspirin's limited solubility. Ethanol (relative polarity 0.654), compatible with aspirin's amphiphilic structure, dissolves it more readily through van der Waals interactions but is less effective in shear transfer. Overall, LAG with ethanol forms a thin liquid-like film due to partial dissolution, surface softening, and powder agglomeration; hence, it is less effective in particle size reduction than other moderately polar liquids we have used (Fig. 3c). Nonpolar liquids like hexane and cyclohexane reduce re-agglomeration by limiting polar interactions, enhancing dispersion through steric effects rather than lattice disruption.[21]

3.2.2 Effect of liquid-to-solid ratio (η). Liquid-assisted grinding (LAG) significantly improved both size and shape due to solvents facilitating surface wetting, reducing interparticle friction, and enhancing fragmentation. The literature shows that optimal nanocrystal formation during LAG typically occurs within an η range of 0.2–0.5, balancing dispersion and particle growth. In this study, η was varied from 0 to 0.4 using different liquids under constant grinding conditions. With distilled water, $\eta = 0.1$ gave the best results producing ~150 nm aspirin nanocrystals with minimal aggregation (Fig. 4c), lower η led to fused particles and higher η caused growth due to reprecipitation. For nonpolar solvents like cyclohexane and

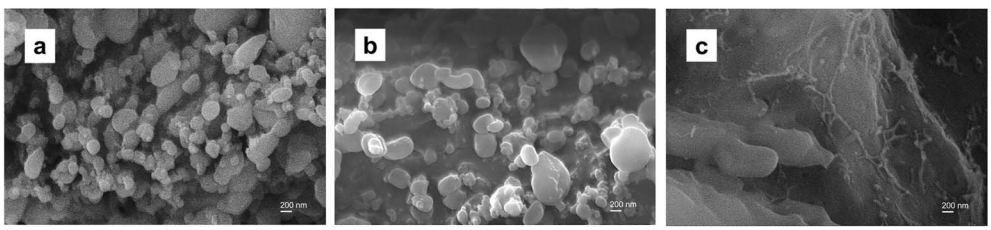

Fig. 3 SEM images of aspirin crystals: (a) ground with cyclohexane at varying η (20 min, 100 μL, 30 Hz, RT 29 °C), (b) ground with hexane (10 min, 100 μL, 30 Hz, RT 29 °C) and (c) ground with ethanol at varying η (60 min, 50 μL, 30 Hz, RT 29 °C).

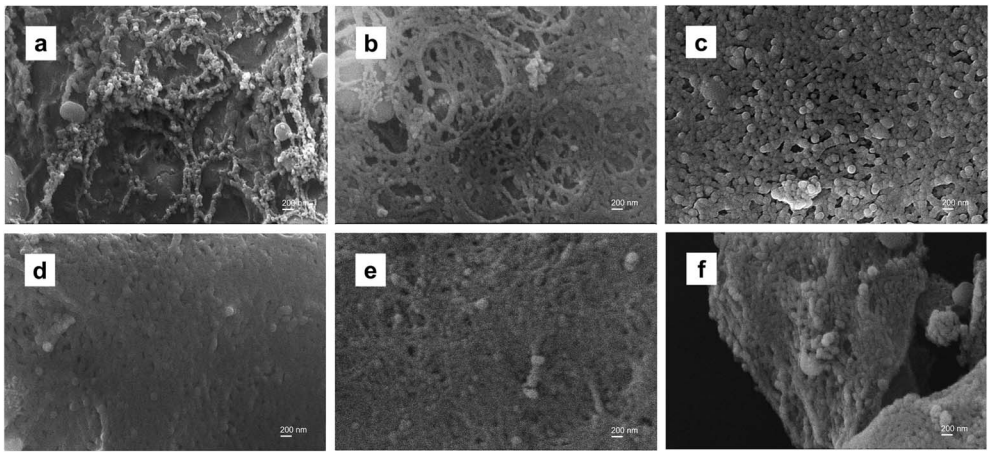

Fig. 4 SEM images of aspirin ground with distilled water at varying milling times: (a) 10 min, 50 μL, 30 Hz, RT 29 °C; (b) 20 min, 50 μL, 30 Hz, RT 29 °C; (c) 30 min, 50 μL, 30 Hz, RT 29 °C; (d) 45 min, 50 μL, 30 Hz, RT 29 °C; (e) 60 min, 50 μL, 30 Hz, RT 29 °C; (f) 75 min, 50 μL, 30 Hz, RT 29 °C.

hexane, $\eta = 0.2$ was optimal, yielding ~200 nm spherical particles (Fig. 3a and b), lower η caused branched shapes from uneven stress, and higher η triggered aggregation due to capillary and coalescence effects. These variations arise from anisotropic growth along high-energy planes exposed during milling; hence, the solvent promotes the layer-by-layer addition of aspirin molecules onto the existing surface, a process favoured both thermodynamically and kinetically.[21] At the nanoscale, surface energy minimization drives the formation of branched or dendritic morphologies.[22] Overall, distilled water at $\eta = 0.1$ proved most effective, highlighting the crucial role of solvent polarity and η in tuning size and morphology.

3.2.3 Effect of milling time. Cyclohexane milling for 20 minutes and hexane for 10 minutes produced more uniform smaller particles. Reduced milling time led to nonhomogeneous crystals with some smaller spherical particles; however, extended milling led to larger crystals due to preferential crystal growth. Water-assisted milling showed strong time dependence. Milling for less than 30 minutes yielded spherical, poorly homogeneous particles exhibit a porous matrix arrangement due to incomplete fragmentation (Fig. 4a and b), while milling for more than 30 minutes improved uniformity through enhanced dispersion. At 45 minutes, particles appeared denser with slight aggregation from re-agglomeration (Fig. 4d–f), due to water-induced plasticization or Ostwald ripening.[23] Optimal milling durations for fine, stable nanocrystals were 30 minutes (water), 20 minutes (cyclohexane), and 10 minutes (hexane).

3.2.4 Effect of grinding frequency on particle size and morphology. Frequencies of 20, 25, and 30 Hz were tested to optimize aspirin nanocrystal formation. At 20 Hz, low energy input led to incomplete nanocrystallization and a mixture of nano- and microparticles (Fig. 5a). Increasing the frequency to 25 Hz reduced the size (~150 nm) but produced porous, irregular structures prone to aggregation (Fig. 5b). At 30 Hz, particles remained at ~150 nm but were more uniform, spherical, and better dispersed, indicating efficient energy transfer and minimized aggregation (Fig. 5c). Thus, 30 Hz emerged as the optimal frequency, yielding stable, well-defined nanocrystals ideal for improved solubility and pharmaceutical performance.

3.2.5 Polymorphic transformation. Aspirin Form IV was synthesized *via* chemical crystallization and mechanochemical milling. While earlier reports described[19] it as metastable and its existence only at 4 °C for 24 hours, our results show that it remains intact at room temperature (26–29 °C) for over 60 days (see SI, Fig. S4), suggesting greater thermodynamic stability than previously thought. When subjected to liquid-assisted grinding (LAG) with water, Form IV consistently transformed into the more stable Form I under various milling conditions (η = 0.2–0.5, time = 10–120 min, and frequency = 20–30 Hz) (Fig. 6a). Water, acting catalytically, enhanced surface mobility and triggered solvent-mediated polymorphic transformation. Its strong hydrogen bonding and surface tension disrupted the Form IV lattice, which induces localized dissolution zones and transient supersaturation at the solid–liquid interface,

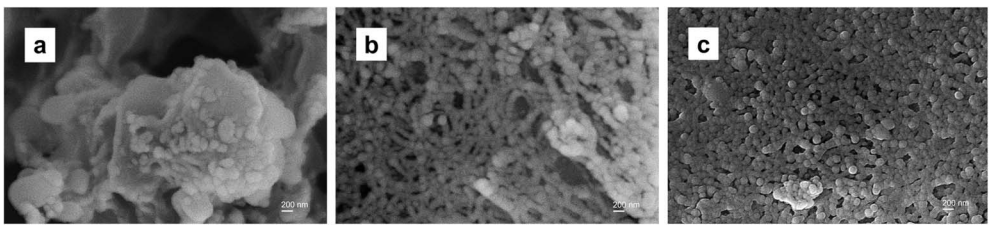

Fig. 5 SEM images of aspirin crystals ground for 30 min (50 μL, RT 26 °C, RH 58.8%) with distilled water at varying frequencies: (a) 20 Hz, (b) 25 Hz and (c) 30 Hz.

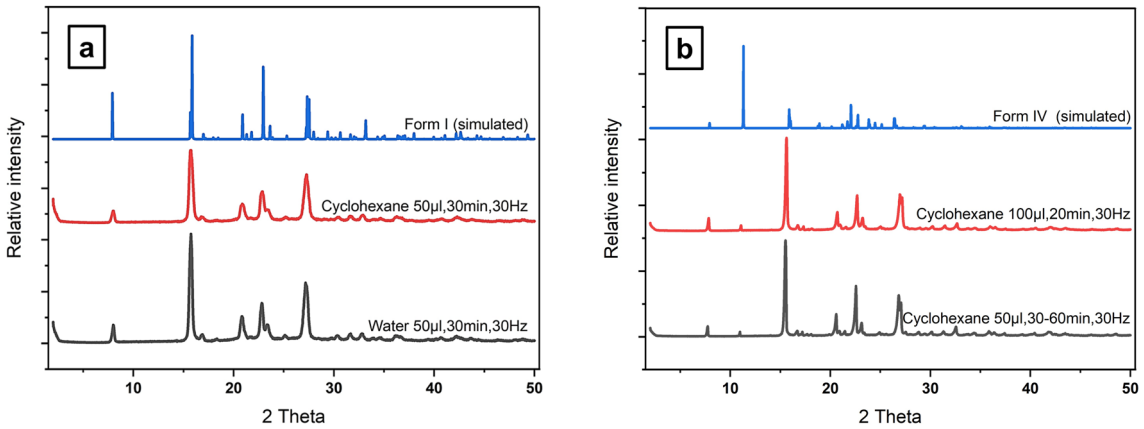

Fig. 6 X-ray powder diffraction patterns of aspirin: (a) Form I simulated (CSD_CIF_ACSALA02), ground with cyclohexane (30 min, 50 µL, 30 Hz, RT 29 °C) and with water (30 min, 50 µL, 30 Hz, RT 29 °C); (b) Form IV simulated (CCDC 1541529), ground with cyclohexane (20 min, 100 µL, 30 Hz, RT 29 °C) and ground with cyclohexane (more than 30 min up to 60 min, 50 µL, 30 Hz, RT 29 °C).

favouring the nucleation of Form I. Even in trace amounts, water accelerates this transformation under suitable thermodynamic and kinetic conditions by promoting molecular rearrangement without full dissolution, consistent with Ostwald's Rule of Stages.[24] With cyclohexane at $\eta = 0.1$, Form IV converts to Form I within 10–30 minutes of grinding but reverts to Form IV after extended grinding (Fig. 6a and b), likely due to kinetic effects like particle size reduction or surface energy shifts. At higher η, Form IV remains dominant, possibly due to reduced mechanical force transmission or stabilization by weak solvent interactions (Fig. 6b). Also, this phase transition, driven by shear stress, proceeds primarily *via* a shear-slip mechanism.[25–27] This highlights how the liquid type, amount, and grinding time govern polymorphic transitions and enable reversible phase control. Although Rietveld refinement was inconclusive, the phase transformation and/or presence of Form IV was characterized based on the presence of a characteristic diffraction peak at $2\theta = 11°$, which is absent in all other polymorphic forms, namely Forms I and II.

3.3 DSC data

The DSC thermogram of bulk Form IV aspirin showed a melting point of around 139.04 °C, indicating a crystalline form likely corresponding to Form IV, as the literature reports melting points of ~144.9 °C for Form I and ~135.5 °C for Form II.[28] The stability order was found to be Form III < IV < II < I,[18,19,29,30] with the increasing stability attributed to various non-covalent interactions such as C–H···π interactions, hydrogen bonding and Gibbs free energy considerations.[31] Typical aspirin Form I melts near 142 °C,[32] though interactions with excipients can alter its degradation path,[33] and rapid cooling may yield an amorphous glass with a T_g of ~244 K.[34] Nano-aspirin samples showed depressed melting points of 118.98 °C (cyclohexane) and 113.90 °C (water) due to particle size reduction[35] (Fig. 7). This size-dependent melting point shift aligns with the Gibbs–Thomson effect, where smaller particles (~200 nm and ~150 nm *vs.* 5–20 µm bulk) melt earlier due to higher surface chemical potential.[36]

3.4 Thermogravimetric analysis

Synthesised aspirin undergoes thermal degradation in two consecutive steps over the temperature range of 120–450 °C.[37] For bulk aspirin (Fig. 8a), the first degradation step occurs with a maximum rate at 198 °C, corresponding to a mass loss of 39.44%. The second degradation step reaches its maximum rate at 369 °C and shows a mass loss of 60.5%, with no residual mass remaining at the end of the analysis. In the case of nano-aspirin (Fig. 8b), the first degradation step is observed at a slightly lower maximum rate temperature of 183 °C, with a mass loss of 42.19%. The second degradation step occurs at a maximum rate temperature of 365 °C and is associated with a mass loss of 57.81%, again leaving no final residue. Thermogravimetric analysis of both bulk and nano-aspirin shows negligible mass loss below the melting temperature range (~135–145 °C), indicating the absence of volatile impurities and confirming the high purity of the samples. The first decomposition step can be attributed to the elimination of acetic acid, resulting from thermally induced cleavage of the ester bond, which is consistent with the characteristic odor observed during heating. The

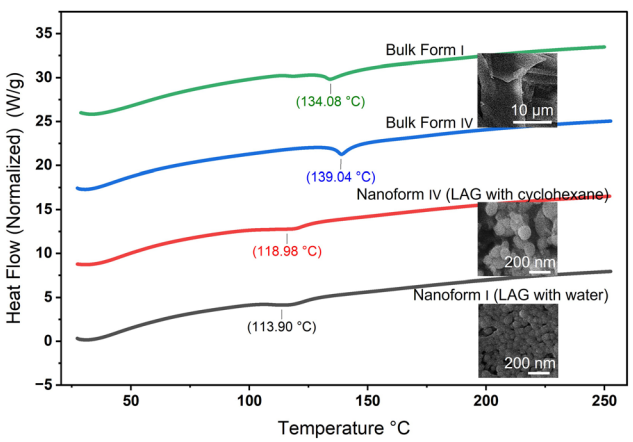

Fig. 7 DSC thermogram for pure aspirin Form I (bulk) 5–20 µm, pure aspirin Form IV (bulk) 5–20 µm, nanoform LAG with water ~150 nm and nanoform LAG with cyclohexane ~200 nm.

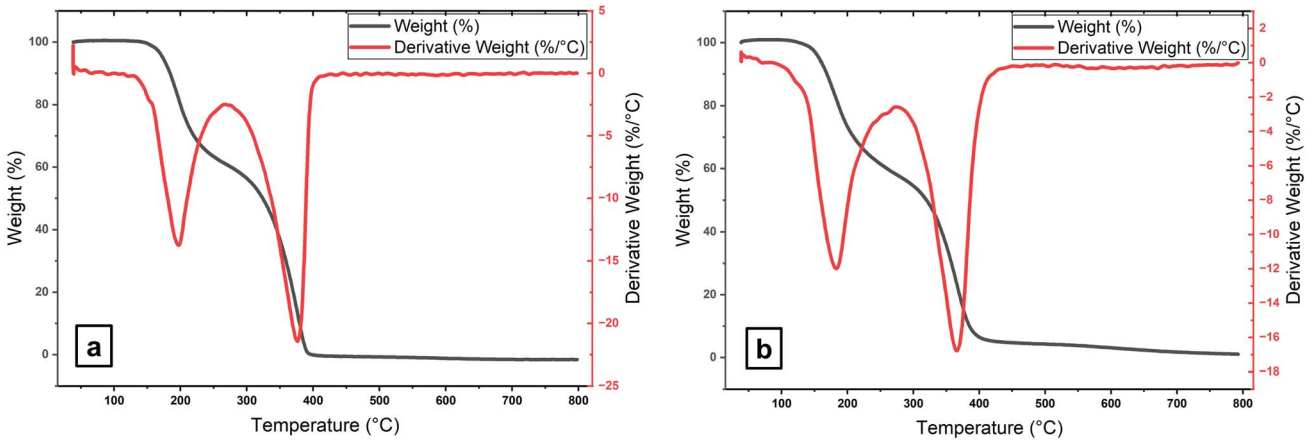

Fig. 8 TGA analysis profiles for (a) aspirin (synthesised) and (b) nanosized aspirin (water ground 30 min, 50 μL, 30 Hz, RT 29 °C).

second step corresponds to the subsequent decomposition of salicylic acid. Bulk and nano-aspirin exhibit similar thermal decomposition profiles and complete mass loss. However, nano-aspirin shows a slightly lower onset temperature for the first degradation step, which can be attributed to increased surface area and enhanced thermal reactivity at the nanoscale.

3.5 Aspirin solubility test

According to the solubility results, both bulk and nanosized aspirin exhibit comparable solubility behaviour, indicating that particle size reduction does not significantly enhance equilibrium solubility under the studied conditions. Furthermore, aspirin shows limited solubility in highly polar protic as well as non-polar solvents. This behaviour can be attributed to the amphiphilic nature of the aspirin molecule, which restricts complete stabilization in solvents of extreme polarity. In contrast, aspirin dissolves more readily in moderately polar solvents, where favourable van der Waals interactions and hydrogen-bonding interactions, together with better structural compatibility between the solute and solvent, promote improved solvation (see SI, Table S1).

3.6 Drug release study

Aspirin nanocrystals showed nearly double the dissolution rate of bulk aspirin at both pH 1.2 and 6.8, with ~90% drug release within 6.5 minutes at pH 1.2 compared to ~50% for the bulk form. Also, nano-aspirin achieved approximately 95% drug release within just 12 minutes at pH 1.2, whereas the bulk form required 56 minutes to reach a similar level of release. This enhancement is due to increased surface area, as explained by the Noyes–Whitney equation.[38] Polymorphism also plays a key role in dissolution. Form I exhibits the slowest release rate due to the dominance of the (001) plane, which forms thinner crystals. Such morphology slows release, as thinner crystals provide less surface area for rapid dissolution. Thus, both polymorphic form and crystal habit[38] significantly impact bioavailability. Metastable forms, though less stable, offer higher surface energy, solubility, and bioavailability. To maximize drug efficacy, solid forms are often ranked for dissolution as amorphous > metastable polymorph > stable polymorph,[1,2,39] with amorphous forms dissolving fastest due to the absence of a crystal lattice. The polymorph form stability order was found to be Form III < IV < II < I.[18,19,29,30] Hence the release rate would

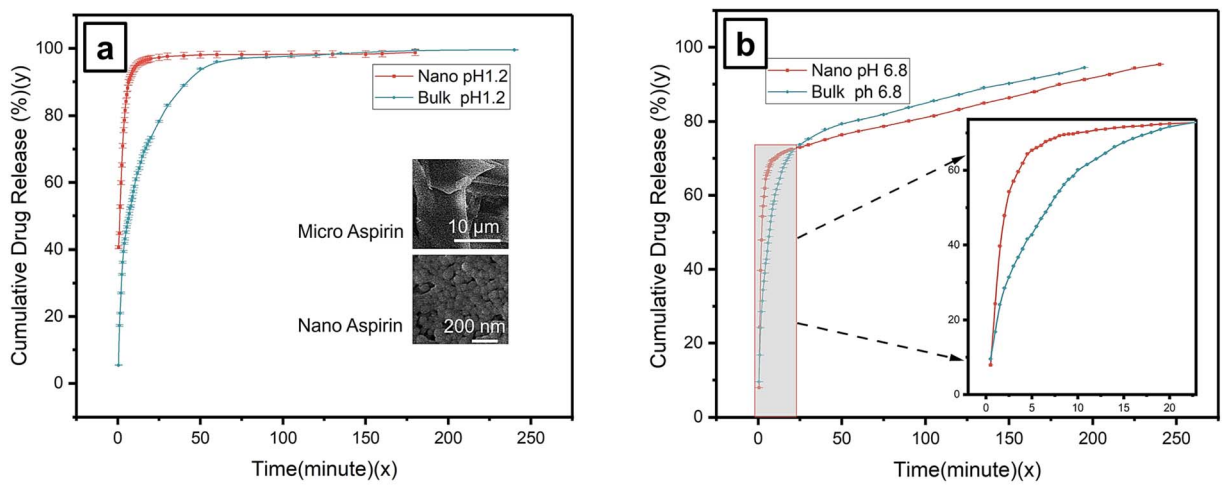

Fig. 9 Aspirin Form I release study of macro- and nanosized particles under (a) pH 1.2 and (b) pH 6.8 simulated gut conditions.

follow the order Form III > Form IV > Form II > Form I. According to our findings, particle size reduction has a greater impact than the polymorphic form. Despite aspirin's greater solubility at pH 6.8 due to ionization (pK_a ~3.5), faster release occurred at pH 1.2, likely because non-ionized aspirin at low pH improves wettability and diffusion. The lower ionic strength of the pH 1.2 buffer (HCl and NaCl) may also favour dissolution by reducing electrical double layer compression, unlike the phosphate buffer at pH 6.8. Recrystallization solvents further impact dissolution by altering crystal habit, especially exposure of the (001) face (Fig. 9).[21,22,31,38]

4 Conclusions

Aspirin nanocrystals were successfully synthesized with excellent homogeneity. Among the tested solvents, distilled water proved to be the most effective medium for LAG, resulting in a particle size of ~150 nm. Hexane and cyclohexane also yielded nanocrystals, with particle sizes of around 200 nm. These results were obtained under milling conditions of high frequency (30 Hz) for 20–30 minutes at approximately 28 °C, with η values between 0.1 and 0.2. This process led to a reduction in the melting point by about 25 °C. Furthermore, our findings reveal that aspirin Form IV can be obtained either through solution crystallization using ethanol and water as solvents or *via* mechanochemical milling using cyclohexane as the LAG medium. In contrast to previous reports that characterized Form IV as metastable and short-lived, our study demonstrates that under the described conditions, this polymorph remains remarkably stable at room temperature (25–29 °C) for a period of over 60 days (see SI, Fig. S4), challenging long-standing assumptions about its thermodynamic behaviour. When water was used as the LAG solvent, milling consistently transformed aspirin Form IV into Form I, which remained stable under all tested conditions. In contrast, using cyclohexane led to the transformation of Form IV into Form I during the first 30 minutes of milling at $\eta = 0.1$. However, extending the milling time to 60 minutes reversed the transformation, converting Form I back into Form IV, and increasing η to 0.2 maintained it in Form IV without further conversion. Moreover, the resulting aspirin nanocrystals exhibited a significantly enhanced dissolution profile compared to bulk aspirin. Notably, under acidic conditions, nearly 90% of the drug was released within just 6.5 minutes. These findings underscore the potential of nanocrystallization to improve the physicochemical properties and therapeutic performance of aspirin, opening new avenues for advanced formulation development.

Conflicts of interest

All the authors declare no conflict of interest.

Data availability

The data supporting this article have been included as part of the supplementary information (SI). Supplementary information: the neat grinding experiment; FTIR spectroscopic analysis; TGA thermogravimetric analysis; PXRD analysis of synthesized aspirin Form IV after 60 days; the aspirin solubility study; the calibration curve for quantitative analysis in the aspirin release study; ferric chloride colorimetric analysis of aspirin; and a comparative evaluation of PXRD patterns obtained from liquid-assisted grinding (LAG) and the initial experimental PXRD data. See DOI: https://doi.org/10.1039/d5mr00118h.

Acknowledgements

N. M. A. is grateful to the University of Peradeniya; University Research Grant 2024 (Grant No. URG/2024/13/E), which supported the procurement of chemicals and characterization activities and Mrs W. M. W. K. Weerasekara at the department instrumental facility is acknowledged. R. T. would like to thank the Polish National Agency for Academic Exchange with application no BNI/ULM/2024/1/00042 to work as a Ulam NAWA fellow at the Faculty of Chemistry, University of Warsaw, Poland. We thank Dr Mihails Arhangelskis (University of Warsaw, Poland) for helpful discussions regarding Rietveld refinement during the revision of the manuscript.

References

1 S. Sareen, L. Joseph and G. Mathew, *Int. J. Pharm. Investig.*, 2012, **2**, 12.
2 M. S. A. Kumar, M. Rajesh and L. Subramanian, *WJBPHS*, 2023, **13**(3), 141–149.
3 M. R. Montinari, S. Minelli and R. De Caterina, *Vascul. Pharmacol.*, 2019, **113**, 1–8.
4 M. Ugurlucan, I. M. Caglar, F. N. Turhan Caglar, S. Ziyade, O. Karatepe, Y. Yildiz, E. Zencirci, F. Gungor Ugurlucan, A. H. Arslan, S. Korkmaz, U. Filizcan and S. Cicek, *Recent Pat. Cardiovasc. Drug Discov.*, 2012, **7**, 71–76.
5 A. Rezabakhsh, A. Mahmoodpoor and H. Soleimanpour, *J. Cardiovasc. Thorac. Res.*, 2021, **13**, 179–180.
6 M. Malamatari, K. M. G. Taylor, S. Malamataris, D. Douroumis and K. Kachrimanis, *Drug Discov. Today*, 2018, **23**, 534–547.
7 I. S. Mohammad, H. Hu, L. Yin and W. He, *Int. J. Pharm.*, 2019, **562**, 187–202.
8 S. J. Shankar, B. H. J. Gowda, R. S. Akshatha, B. Metikurki and M. Rehamathulla, *Int. J. Appl. Pharm.*, 2019, 10–16.
9 M. Kumar, N. Shanthi and A. K. Mahato, *Nanosci. Nanotechnol. - Asia*, 2019, **9**, 300–310.
10 S. N. Madanayake, A. Manipura, R. Thakuria and N. M. Adassooriya, *Org. Process Res. Dev.*, 2023, **27**, 409–422.
11 T. Friščić, *J. Mater. Chem.*, 2010, **20**, 7599.
12 D. Tan, L. Loots and T. Friščić, *Chem. Commun.*, 2016, **52**, 7760–7781.
13 J. L. Ferreira da Silva, M. F. Minas da Piedade, V. André, S. Domingos, I. C. B. Martins and M. T. Duarte, *Molecules*, 2020, **25**, 2705.
14 D. G. Ramanan, R. T. Bandara, R. Thakuria and N. M. Adassooriya, *CrystEngComm*, 2025, **27**, 2260–2280.
15 M. Alrbaihat, *Adv. Mat. Res.*, 2023, **1175**, 37–46.

16 P. Vishweshwar, J. A. McMahon, M. Oliveira, M. L. Peterson and M. J. Zaworotko, *J. Am. Chem. Soc.*, 2005, **127**, 16802–16803.
17 A. D. Bond, K. A. Solanko, S. Parsons, S. Redder and R. Boese, *CrystEngComm*, 2011, **13**, 399–401.
18 E. L. Crowell, Z. A. Dreger and Y. M. Gupta, *J. Mol. Struct.*, 2015, **1082**, 29–37.
19 A. G. Shtukenberg, C. T. Hu, Q. Zhu, M. U. Schmidt, W. Xu, M. Tan and B. Kahr, *Cryst. Growth Des.*, 2017, **17**, 3562–3566.
20 T. Dong, E. P. Knoshaug, P. T. Pienkos and L. M. L. Laurens, *Appl. Energy*, 2016, **177**, 879–895.
21 T. Li, B. Li and M. S. Tomassone, *Chem. Eng. Sci.*, 2006, **61**, 5159–5169.
22 B. P. A. Gabriele, C. J. Williams, D. Stauffer, B. Derby and A. J. Cruz-Cabeza, *Cryst. Growth Des.*, 2021, **21**, 1786–1790.
23 C. C. Yec and H. C. Zeng, *J. Mater. Chem. A*, 2014, **2**, 4843–4851.
24 P. T. Cardew, *Cryst. Growth Des.*, 2023, **23**, 3958–3969.
25 S. Varughese, M. S. R. N. Kiran, K. A. Solanko, A. D. Bond, U. Ramamurty and G. R. Desiraju, *Chem. Sci.*, 2011, **2**, 2236.
26 L. M. LeBlanc, A. Otero-de-la-Roza and E. R. Johnson, *Cryst. Growth Des.*, 2016, **16**, 6867–6873.
27 S. Varughese, M. S. R. N. Kiran, K. A. Solanko, A. D. Bond, U. Ramamurty and G. R. Desiraju, *Chem. Sci.*, 2011, **2**, 2236.
28 P. Peksa, J. Trzmiel, M. Ptak, M. Kostrzewa, R. Szatanik, A. Barascu, D. Enke and A. Sieradzki, *J. Mater. Sci.*, 2019, **54**, 404–413.
29 A. M. Reilly and A. Tkatchenko, *Phys. Rev. Lett.*, 2014, **113**, 055701.
30 A. D. Bond, K. A. Solanko, S. Parsons, S. Redder and R. Boese, *CrystEngComm*, 2011, **13**, 399–401.
31 Y. Vaksler, A. Idrissi, V. V. Urzhuntseva and S. V. Shishkina, *Cryst. Growth Des.*, 2021, **21**, 2176–2186.
32 G. T. Long, S. Vyazovkin, N. Gamble and C. A. Wight, *J. Pharm. Sci.*, 2002, **91**, 800–809.
33 D. J. Ager, K. S. Alexander, A. S. Bhatti, J. S. Blackburn, D. Dollimore, T. S. Koogan, K. A. Mooseman, G. M. Muhvic, B. Sims and V. J. Webb, *J. Pharm. Sci.*, 1986, **75**, 97–101.
34 G. P. Johari and D. Pyke, *Phys. Chem. Chem. Phys.*, 2000, **2**, 5479–5484.
35 X.-H. Sui, Z.-G. Wang, K. Kang, S.-J. Qin and C.-L. Wang, *Commun. Theor. Phys.*, 2015, **63**, 249–254.
36 M. PEREZ, *Scr. Mater.*, 2005, **52**, 709–712.
37 H. M. Al-Maydama, A. A. Abduljabbar, M. A. Al-Maqtari and K. M. Naji, *J. Mol. Struct.*, 2018, **1157**, 364–373.
38 A. Watanabe, Y. Yamaoka and K. Takada, *Chem. Pharm. Bull.*, 1982, **30**(8), 2958–2963.
39 K. Yadav, A. Kr. Sachan, S. Kumar and A. Dubey, *Asian J. Pharm. Res. Dev.*, 2022, **10**, 144–153.